

Imperial College London  
Department of Earth Science and Engineering  
MSc in Applied Computational Science and Engineering

Independent Research Project  
Final Report

# Seagrass mapping using satellite data on Google Earth Engine

by  
Siyu Wang

siyu.wang19@imperial.ac.uk  
GitHub login: acse-ws4418

Supervisors:  
Professor Piggott, Matthew D  
Plancherel, Yves

August 2020

## **Abstract**

Seagrass plays an important role in maintaining marine biodiversity, marine ecology and even the global environment. The objective of the project is to develop a workflow based on the Google Earth Engine (GEE) platform that can map and monitor seagrass habitats using optical satellite remote sensing data. To achieve this, the region around Lemnos Island in the north part of the north Aegean Sea is selected due to the availability of field data that can be used for validation and the abundance of *Posidonia* seagrass growing off the eastern coast of Lemnos. Key novelties of this work are the use of GEE to develop a complete mapping workflow and the subsequent comparison of three machine learning methods. This project also emphasizes the importance of seagrass protection and calls on humans to use different methods to protect seagrass from different threats, thereby helping to protect the global environment.

**Keywords:** Seagrass, Lemnos, Google Earth Engine, Global environment

## 1. Introduction

Seagrasses are plants living in the water and play significant ecological roles in the coastal ecosystem because they can form broad habitats near the continental shelf (Traganos et al.; 2018a, Traganos et al., 2018b). In this area, other species are benefiting from the nutrients provided by seagrasses. Meanwhile, seagrass meadows can prevent excessive erosion and absorb the greenhouse gas via photosynthesis, which reduces 15% of the ocean's carbon (Traganos et al., 2018; Nordlund, 2016). In that way, they make a huge contribution to the biodiversity and element balance of the ecosystem. Furthermore, the content of organic matter produced by seagrasses is far more than the amount of organic matter needed for their growth, so they can mitigate the impact of climate change (Traganos et al.; 2018).

In the north Aegean Sea, there are one of the most important oxygen sources from the ecosystem, *Posidonia oceanica* seagrass. This kind of seagrass distributed around the coast of the north Aegean Sea in sheltered areas such as harbours, estuaries, lagoons, and bays. *Posidonia oceanica* in the North Aegean Sea is declining drastically because of human activities such as reclamation, over-fishing, construction, boating, dredging, tourism, and sewage with high nutrients. The amount of *Posidonia oceanica* decrease by 10% compared with the last 100 years (MedWet, 2017). This situation is more significant in urbanized areas, which may increase the content of heavy metal elements in the seawater around these areas. Seagrasses can reduce the speed of water flow and allow heavy metal elements to accumulate in their body (The Wildlife Trust, 2020). As the accumulation of heavy metal elements increases, the seagrass's ability to fix nitrogen will decrease, thereby reducing its viability. In the past few decades, 30,000 km<sup>2</sup> of seagrass has been lost globally, which is equal to 18% of the global area (The Wildlife Trust, 2020). So, protecting seagrass is one of the most important environmental problems we need to solve.

Globally, there are treaties related to the protection of sustainable development, and also aspirational goals for the protection of seagrass habitats such as the Sustainable Development Goals (SDG) of the UN's 2030 Agenda for Sustainable Development and "Protocol concerning Specially Protected Areas and Biological

Diversity in the Mediterranean" (Traganos et al.; 2018). These measures are designed to protect the world's seagrass and thus protect the environment from climate change.

With more applications of optical and computer disciplines, the mapping of seagrass no longer depends on traditional methods like field trips. Optical satellite remote sensing is a convenient method used to map and monitor seagrasses. From the images of the satellite, it is easy to get the reflectance of each pixel at different wavelengths, which is called a spectrum of the pixel. The spectral characteristics of each type of substance are different, so it is probably to use this feature to find the distribution of the seagrasses in the remote sensing image and then apply analysis on it. This is the basic principle of mapping seagrasses based on remote sensing images. However, the use of satellite remote sensing for large-scale mapping lacks in-situ data. Such data is often not as remote sensing data with a high time activity and covers a relatively small range. In the existing in-situ data sets, only a few data sets can provide valuable spatial information for image analysis (Traganos et al.; 2018). Mapping seagrasses faces other challenges such as the lack of extensive records of seagrass species diversity and changes in water quality over time, which may affect the accuracy of the extraction of seagrass information (Traganos et al.; 2018).

In the past, large-scale seagrass mapping mainly used Landsat satellite data on the local scale. However, with the innovation of cloud computing and big data technology, cloud platforms like Google Earth Engine (abbreviated as GEE) have emerged. GEE is a cloud computing platform that can store, process, and analyse many datasets. It is open source so users can access the dataset conveniently (Mutanga & Kumar, 2019). GEE integrated various remote sensing datasets from different satellites and can also store geographic information data such as vector boundaries and weather. Users are also allowed to create their datasets. GEE can be applied in vegetation mapping and monitoring, disaster management, landcover mapping, and earth science related applications (Mutanga & Kumar, 2019). For instance, researchers have produced the status and distribution of forests on a global scale and have mapped the cropland in Africa.

The aim of the project is the development of an end to end workflow to map the seagrass in specific study area Lemnos and can be extended to the global scale. There is also an assessment of the accuracy of different classification techniques.

## 2. Study Area

The study area is the island of Lemnos, in the north part of the Aegean Sea. *Posidonia Oceanica* grows on the northeast of the Lemnos. The area of the island is 476 square kilometres.

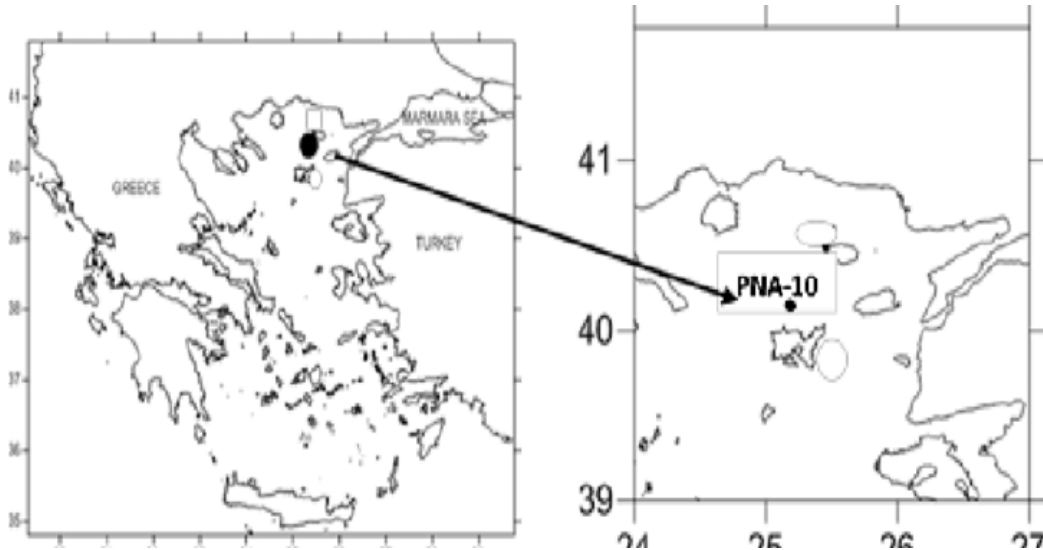


**Figure 1.** Geographical location of the study area Lemnos in north Aegean Sea (Pappa et al., 2019)

## 3. Data source

### 3.1. Remote sensing Data

The remote sensing image that will be used in this study comes from the Sentinel-2 multispectral instrument in the GEE platform, which has been atmospherically corrected. There are twin polar-orbiting which are Sentinel-2A launched on 23 June 2015 and Sentinel-2B launched on 07 March 2017. Sentinel-2 consists of 13 bands with b1-coastal aerosol, b2-blue, b3-green, b4-red, b5.6.7-vegetation red edge, b8-NIR, b8A-vegetation red edge, b9-water vapour, b10.11.12-SWIR. Band1, band9, and band 10 are 60m spatial resolution, while band 5, 6, 7, 8A, 11, and 12 are 20m spatial resolution, and band 2, 3, 4, 8 are 10m spatial resolution. Sentinel-2 can be used to detect vegetation growth, soil coverage to evaluate the environment of the detected area. It is not only important for planning the forestry, predicting grain output, and ensuring food security but can also be used to monitor natural disasters such as landslides, floods, and volcanic eruptions to aid with humanitarian relief.

### 3.2. Training Data

The training data are collected through digitization from the high-resolution base map and the Landsat image of the Lemnos. 1604 unified digital points are collected by hand selection, and 1001 digital points are represented as seagrass, 101 digital points as shallow water and, 503 digital points as deep water. Seagrass's label is configured as 0, shallow water label as 1 and deep water as 2.

**Table 1.** The number of training data.

Class	Points	%
Seagrass	1001	62.4
Shallow water	101	6.3
Deep water	503	31.3

### 3.3. Validation data

The field trip data records are collected from the Natura 2000 network website ([https://ec.europa.eu/environment/nature/natura2000/index\\_en.htm](https://ec.europa.eu/environment/nature/natura2000/index_en.htm)) published by the European Union. There are 62 coastal areas in this network and the Lemnos site is coded as GR110001. The seagrass area of GR110001 is recorded as 115.07 km<sup>2</sup> and this figure can be used in the result accuracy assessment.

## 4. Software Description

The whole solution is developed as a standalone code with the use of effective API from Google Earth Engine. The process is divided into three parts which are pre-processing, classification, and accuracy assessment. The figure below depicts the development methodologies used and the architectural design.

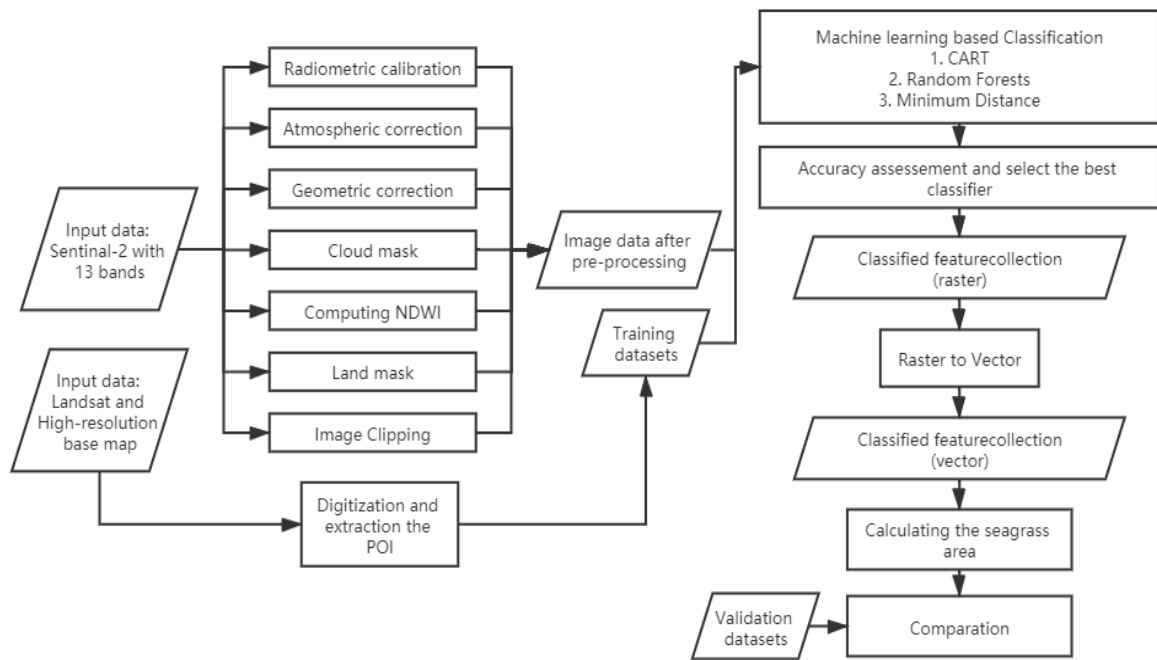


**Figure 2.** Methodological workflow (made by processon) based on the Google Earth Engine.

#### 4.1. Pre-processing

Seven steps are included in the pre-processing part and the first three step has been done from the dataset of GEE but these steps are the most important parts in general image pre-processing:

1. Radiometric calibration: This step is to convert the recorded Digital Number value from the satellite into the reflectance of the top of the atmosphere. Different sensors from satellites have different radiometric calibration formula. This conversion process is generally completed by a linear relationship:

$$L_{\lambda} = Gain \cdot DN + Offset \quad (1)$$

2. Atmospheric correction: This step is to convert the radiance to the reflectance of the top of the atmosphere and then convert the reflectance of the top of the atmosphere to the ground surface reflectance to eliminate the errors caused by atmospheric scattering, absorption, and reflection. The apparent reflectance of the atmosphere (reflectance of the top of the atmosphere) can be obtained by the following formula:

$$\rho_{\lambda} = \frac{\pi L_{\lambda} d^2}{ESUN_{\lambda} \sin \theta} \quad (2)$$

Symbols	Definition
$L_{\lambda}$	Radiance in units of W/(m <sup>2</sup> * sr * μm)
$d$	Earth-sun distance, in astronomical units.
$ESUN_{\lambda}$	Solar irradiance in units of W/(m <sup>2</sup> * μm)
$\theta$	Sun elevation in degrees

Because this study is a quantitative study on the area of seagrass, the radiation transmission model is chosen to perform the atmospheric correction. Radiation transmission models include MORTAN models, LOWTRAN model, ATCOR model, and 6S model, etc.

3. Geometric Correction: Geometric correction is the process of correcting geometric distortion caused by system and non-system reasons to make the image conform to the map projection. Changes in the position and movement of the remote sensing platform, topography, surface curvature, atmospheric refraction, and rotation of the earth will cause geometric distortion. Commonly used geometric correction methods are the polynomial method, collinear equation method, rational function method, and small facet differential correction method based on automatic registration. Fortunately, the Sentinel 2 image from GEE has helped us complete the geometric correction.
4. Cloud mask: Because the cloud in the image may affect our interpretation of the images, the cloud mask is needed. QA60 bitmask band from Sentinel 2 is used to mask the cloud and cirrus.
5. Computing NDWI: The full name of NDWI is normalized difference water index and it is an improved version of WI used to extract water area from a satellite image. The formula of NDWI is:

$$NDWI = \frac{Green\ band - NIR\ band}{Green\ band + NIR\ band} \quad (3)$$



Symbols	Definition
<i>Green band</i>	Green band: B3 in Sentinel 2
<i>NIR band</i>	Near infrared band: B8

Through this step, water bodies in the image can be extracted and be prepared for the next step land mask.

6. Land mask: Seagrass is growing in the water when performing machine learning classification, the land part of the image can be masked out, which can improve the computational efficiency. The land area is digitized by hand from the NDWI result.
7. Image clipping: After the land mask, the land area vector is used to clip the image and obtain the image with only shallow water, deep water, and seagrasses.

#### 4.2. Classification

In the classification part, three different supervise classifications are considered, which are CART classification, random forest classification, and minimum distance classification. The method with the highest accuracy for the seagrass classification and the best effect is selected.

##### 4.2.1. CART classification

CART is the abbreviation of "Classification and Regression Trees", which means "Classification and Regression Trees". It is divided into CART generation algorithm and CART pruning algorithm. The generation algorithm corresponds to classification and regression. The prediction method of the classification tree is that the category with the highest probability in the leaf node is used as the predicted category of the current node, and the prediction method of the regression tree is to use the y mean value of the sample in the leaf node as the predicted value of the regression.

The regression tree uses the RSS residual sum of squares. The formula is as follows:

$$\min_{j,s} \left[ \min_{c_1} \sum_{x_i \in R_1(j,s)} (y_i - c_1)^2 + \min_{c_2} \sum_{x_i \in R_2(j,s)} (y_i - c_2)^2 \right] \quad (4)$$

Symbols	Definition
$c_1 c_2$	Representative values of the two regions
$j$	Optimal segmentation variable
$s$	Split point

The purpose of the formula is to calculate the sum of the residual squares of all the features and the corresponding segmentation points and find a set to minimize the sum of squares of residuals of the left subtree and the right subtree respectively and minimize the sum of the two again.

In summary, the advantages of the CART method are simple and intuitive. It also has good fault tolerance for abnormal points and high robustness tree. The disadvantage is that the CART algorithm is very easy to overfit, resulting in poor generalization ability.

#### 4.2.2. *Random forest classification*

Random forest is a highly flexible machine learning algorithm. Like decision trees, random forests can be used for both regression and classification. The basic unit is a decision tree. So, in theory, the results of random forests are generally better than the results of decision trees, because the results of random forests are determined by voting on the results of multiple decision trees. Compared with all current machine learning classification algorithms, it has extremely high accuracy and can process large data sets. In the process of generating a random forest, an unbiased estimate of the internal generation error can be obtained. Random forest does not need to do a lot of parameter tuning like other classification algorithms.

#### 4.2.3. *Minimum distance classification*

The minimum distance method is an easy classification method in machine learning classification methods. Compared with CART and Random Forest, the principle of this method is simpler and the calculation speed is faster, but it does not consider as many factors as the other two methods, so the classification accuracy is not high. But the results obtained by this method can be used as a comparative experimental group to assist in verifying the results.

### 4.3. Accuracy assessment

Accuracy assessment consists of two parts. The first part is the accuracy assessment of the classification method. 75% of the digitally extracted seagrass polygon data is used as the training set and 25% is used as the validation set. Through the confusion matrix, the final classifier used is determined. The second part is to compare the seagrass area finally obtained by the whole solution with the field data obtained from the Natura 2000 network.

## 5. Code Metadata

JavaScript is used as the coding language for the whole process. The entire development process is implemented in the Code Editor from the GEE platform, as shown in the figure below.

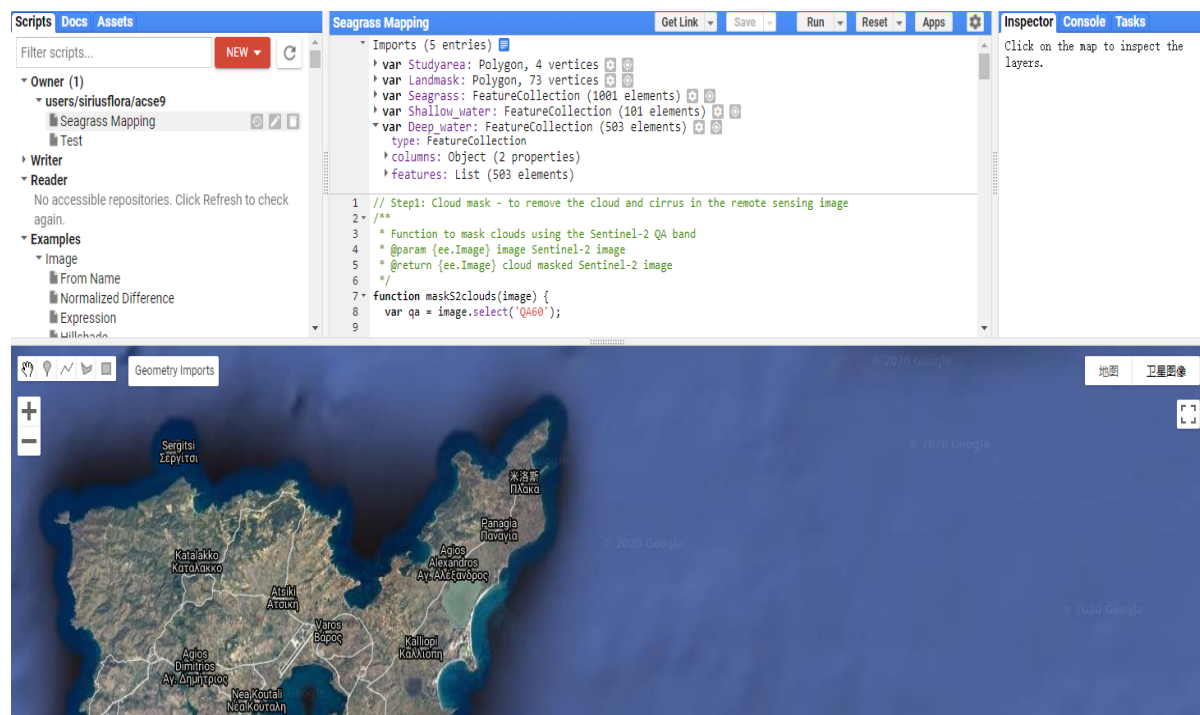


**Figure 3.** The user interface of Code Editor in GEE.

The Code Editor user interface can be divided into four parts: script file storage area, code editing area, output console, and result map display area.

- 1) Script file storage area: All code files are stored here, including self-created and Google official sample codes. It also supports the creation of folders and new files.
- 2) Code editing area: This area is the main code implementation area. Almost all development work is completed in this area. Click "Save" to save the file to the cloud, and click "Run" to run the script.
- 3) Output console. When running the script, all print content will be displayed in this area.
- 4) Map display area. This area is where the geographically related results will be displayed based on the Google Map.

**Table 2.** The links of code and support document












Link	
GitHub	<a href="https://github.com/acse-2019/irp-acse-ws4418.git">https://github.com/acse-2019/irp-acse-ws4418.git</a>
Support documents	<a href="https://developers.google.com/earth-engine">https://developers.google.com/earth-engine</a>

## 6. Implementation and Code

The entire code contains five major blocks, namely data import, data pre-processing, machine learning classification, accuracy verification, and statistical calculation.

### 6.1. Data import

This part describes the input, output, and functions of the code block. The data input includes Study area Polygon, Land mask Polygon, and three Feature Collection of POI for training.

```
Imports (5 entries)   
▼ var Studyarea: Polygon, 4 vertices    
  type: Polygon  
  ▶ coordinates: List (1 element)  
  geodesic: false  
  ▶ var Landmask: Polygon, 73 vertices    
  ▶ var Seagrass: FeatureCollection (1001 elements)    
  ▶ var Shallow_water: FeatureCollection (101 elements)    
  ▶ var Deep_water: FeatureCollection (503 elements)  
```

**Figure 4.** The input data of the programme in different data type.

GEE can integrate the input data into a module, and the internal situation including data types, attributes, coordinates of the elements in the data can be checked without running the programme. The imported data can also be displayed visually in Google Maps in GEE.

## 6.2. Data pre-processing

Cloud mask, land mask, and the calculation of NDWI are introduced in this part. For cloud mask, which aims to remove the cloud and cirrus in the Sentinel-2 image, a function called maskS2clouds is created. The input parameter is the Sentinel-2 image and returns the cloud masked Sentinel-2 image. BitwiseAnd API is used to filter the QA60 band because it can calculate the bitwise AND of the input values for each matched pair of bands in two images. For cloud and cirrus, both flags should be set to zero, indicating clear conditions as shown in the code block below.

```
function maskS2clouds(image) {  
  var qa = image.select('QA60');  
  
  // Bits 10 and 11 are clouds and cirrus, respectively.  
  var cloudBitMask = 1 << 10;  
  var cirrusBitMask = 1 << 11;  
  
  // Both flags should be set to zero, indicating clear conditions.  
  var mask = qa.bitwiseAnd(cloudBitMask).eq(0)  
    .and(qa.bitwiseAnd(cirrusBitMask).eq(0));  
  
  return image.updateMask(mask).divide(10000);  
}
```

**Figure 5.** The function of cloud mask using bitwiseAnd API in GEE.

Then, the function created above is used in the filter of the dataset. The filterDate API can filter the period of the image, here is set to 2019.01.01 to 2020.07.01. According to the property 'CLOUDY\_PIXEL\_PERCENTAGE', it is easy to obtain less cloudy granules with the figure lower than 20. After mapping the function created above and get the mean values, the filtered dataset is a dataset with cloud clear images.

```
// Filter the image without cloud using the function above
var dataset = ee.ImageCollection('COPERNICUS/S2_SR')
                .filterDate('2019-01-01', '2020-07-01')
                // Pre-filter to get less cloudy granules.
                .filter(ee.Filter.lt('CLOUDY_PIXEL_PERCENTAGE',20))
                .map(maskS2clouds).mean();

var clipped_dataset = dataset.clip(Studyarea);
```

**Figure 6.** The filter of cloud and date.

The next step is to compute the NDWI using an expression to extract the land region in the image and then digitize the land mask for the image clipping. Expression API can evaluate an arithmetic expression on an image. It also specifies the multiple bands such as green refers to 'B3'. The function returns the image computed by the provided expression. The land area can be easily extracted from the NDWI image.

```
var ndwi = clipped_dataset.expression(
  '(green - nir) / (green + nir)',
  {
    green: clipped_dataset.select('B3'), // Green band
    nir: clipped_dataset.select('B8'),   // Near infrared band
  });
```

**Figure 7.** The code block of computing NDWI using an expression.

The figure below is the result of the NDWI. The land is set to black with a white boundary.

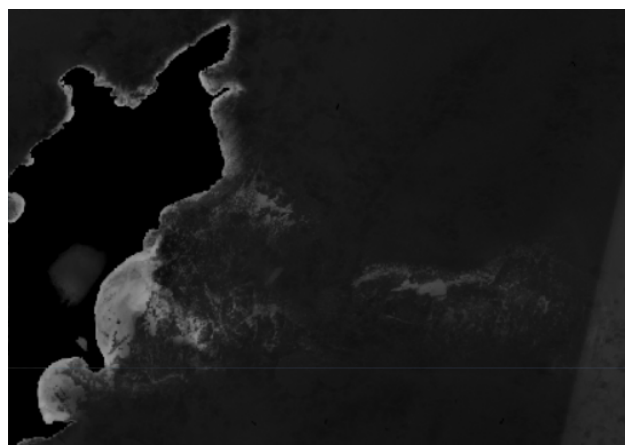


**Figure 8.** The result of the NDWI.

### 6.3. Classification

The next step is to train the model, using three classification methods to train the three models. The principles of the three classification methods have been introduced in the software description.

```
// 1. CART classifier.
var classifier_Cart = ee.Classifier.smileCart().train({
  features: training,
  classProperty: classProperty,
});

// Print some info about the classifier (specific to CART).
print('CART, explained', classifier_Cart.explain());

// Classify the composite.
var classified_Cart = masked_dataset.classify(classifier_Cart);
Map.centerObject(roi);
Map.addLayer(classified_Cart, {min: 0, max: 2, palette: ['green', '#00ffff', 'blue']});
```

**Figure 9.** Training the CART classifier.

Three classification results are shown in the figure below.

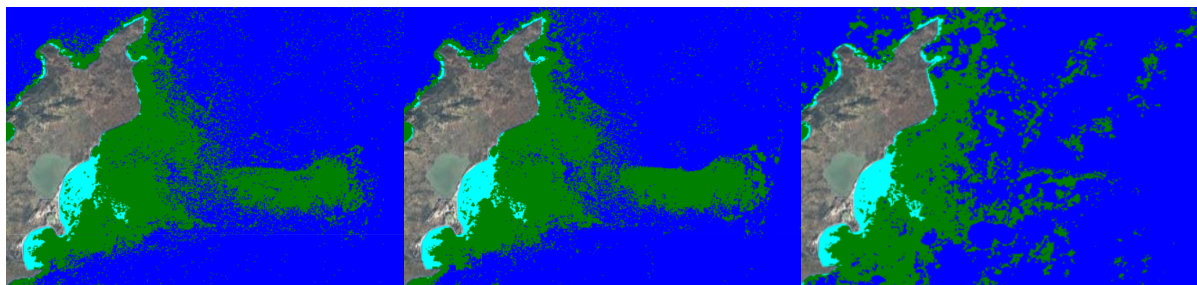


**Figure 10.** The classification results of CART, Random Forest, and Minimum Distance

### 6.4. Accuracy assessment

In order to choose the best classifier, the confusion matrix is a good indicator of accuracy. The data is split by 75% for training and 25% for testing. First, create a set of pseudo-random numbers using randomColumn API, and divide the data randomly through this set. Then, calculate the confusion matrix of three classification results, and display the matrix in the console.

```
// Add a column of random uniforms to the training dataset.
var withRandom = training.randomColumn('random');

// We want to reserve some of the data for testing, to avoid overfitting the model.
var split = 0.75; // Split the data of 75% for training, 25% for testing.
var trainingPartition = withRandom.filter(ee.Filter.lt('random', split));
var testingPartition = withRandom.filter(ee.Filter.gte('random', split));

// 1. Assessment of CART
var trainedClassifier_CART = ee.Classifier.smileCart().train({
  features: trainingPartition,
  classProperty: classProperty,
  inputProperties: bands
});

// Classify the test FeatureCollection.
var test_CART = testingPartition.classify(trainedClassifier_CART);

// Print the confusion matrix.
var confusionMatrix_CART = test_CART.errorMatrix(classProperty, 'classification');
print('Confusion Matrix of CART', confusionMatrix_CART);
```

**Figure 11.** Test the accuracy of the classifiers.

Confusion matrix is a suitable method to test the accuracy of the classification. The seagrass classification accuracy is 93.19%, 93.19%, and 59.15% respectively.

**Table 3.** The confusion matrix of CART classifier.

	Seagrass	Shallow water	Deep water	Accuracy
Seagrass	219	1	15	93.19%
Shallow water	0	20	0	100%
Deep water	15	0	114	88.37%

**Table 4.** The confusion matrix of Random Forest classifier

	Seagrass	Shallow water	Deep water	Accuracy
Seagrass	219	0	16	93.19%
Shallow water	0	20	0	100%
Deep water	7	0	122	94.57%

**Table 5.** The confusion matrix of Minimum Distance classifier

	Seagrass	Shallow water	Deep water	Accuracy
Seagrass	139	1	95	59.15%
Shallow water	0	20	0	100%
Deep water	25	0	104	80.62 %

The final step is to calculate the seagrass area from the best result of three classifiers. Random forest has the highest overall accuracy so this method is chosen to calculate



the seagrass area. The poor effect of the minimum distance method may be due to the uneven distribution of the number of samples. First, `reduceToVectors` API is used to convert the classified raster data into vector data to calculate the area. Then use `map` function to compute the area of each vector, the unit is square meters, and add them to the properties. In this way, A new property called 'area' will be set on each feature. Finally, the `aggregate_sum` function is used to calculate the sum of the area of all appropriate units, and the final result is 112.59km<sup>2</sup>.

```
// Convert the raster to vector.
var vector = classified_Rf.reduceToVectors({
  scale:100,
});

// Filter the seagrass from the vector.
var seagrass_vector = vector.filterMetadata('label','equals',0);
Map.addLayer(seagrass_vector);
print(seagrass_vector);

// Compute the area and add as a property to the vector.
var SeagrassWithArea = seagrass_vector.map(function(f) {
  // Compute area in square meters.
  var areaHa = f.area(10);

  // A new property called 'area' will be set on each feature.
  return f.set({area: areaHa});
});

print(SeagrassWithArea);

// Compute the summary of the seagrass area in the study area.
var area_of_seagrass = SeagrassWithArea.aggregate_sum('area');
print(area_of_seagrass);
```

**Figure 12.** Seagrass area calculation.

## 6.5. Test on another site

Finally, another site Western Greece is selected to test the whole workflow. 64.3 km<sup>2</sup> seagrass is detected by the workflow. The record from the field trip is 51.54 km<sup>2</sup>. The bias is 8.8 km<sup>2</sup>. Similarly, three classification methods are performed on the study area. The classification with the best result (also random forest) is shown below.

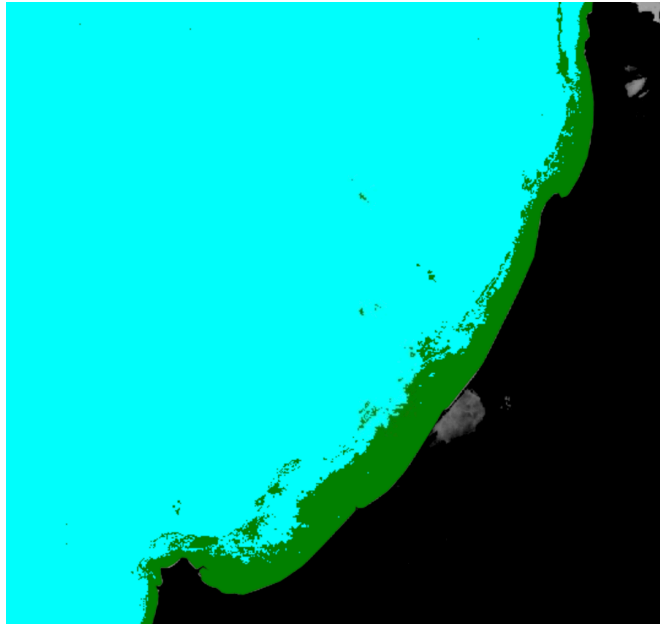


**Figure 13.** The Random forest classification result of Western Greece.

## 7. Discussion and Conclusions

### 7.1. Conclusion

This study takes Lemnos in the northern Mediterranean as the research area and develops a seagrass mapping workflow based on the Google earth engine platform. The input data and the choice of POI can be adjusted freely. 112.59km<sup>2</sup> of seagrass was drawn from the sea area of 130.09km<sup>2</sup> in Lemnos. The field trip record from Natura 2000 is 115.07km<sup>2</sup>. There is only an error of 2.48km<sup>2</sup>. Another site in Western Greece is tested with a high accuracy and only 8.8km<sup>2</sup> bias. In summary, this workflow probably can be extended to the automatic drawing and monitoring of seagrass on a large scale or even globally, but this could be species-specific. In this way, the areas where the area of seagrass continues to be reduced will be protected specifically and will ultimately provide support for global ecological protection.

### 7.2. Limitation

The water depth, the sun's altitude angle, and the clarity of the water body will all have an impact on the classification results, and this workflow does not consider the above three elements. Seagrass with water depth greater than 40m is often difficult to detect, and what can be detected often corresponds to very high visibility. Besides, because

Sentinel-2 images are acquired from different angles, stripes will appear, which will also affect the classification results (Topouzelis et al.; 2017). For instance, visibility may infect the seagrass recognition by eyes.

### 7.3. Future work

For seagrass monitoring in different regions, the parameters and data pre-processing might be adjusted according to local conditions (Topouzelis et al.; 2017). Also, the entire data pre-processing of the seagrass mapping workflow can be structured and systematized, such as unified water depth correction, standardized processes for water turbidity correction. At the same time, with the development of open-source data and satellite technology, the spatial resolution of public remote sensing images may be higher in the future, which is more conducive to the drawing of seagrass, to protect the marine ecological environment more conveniently and accurately.

## Acknowledgments

First of all, I would like to extend my sincerest thanks to my professors Piggott, Matthew D, and Plancherel, Yves. They give me great help in the completion of my project, including project introduction, revising the project plan, the mid-term routine meeting, and the final report revision. I also thank my team members. When we encounter problems, we will discuss and communicate with each other and find solutions. Finally, I would like to thank my parents. They always understand me, support me, and give me great encouragement.

## References

1. Mutanga, O.; Kumar, L. Google Earth Engine Applications. *Remote Sens.* **2019**, *11*, 591.
2. Nordlund, M.L.; Koch, E.W.; Barbier, E.B.; Creed, J.C. Seagrass Ecosystem Services and Their Variability across Genera and Geographical Regions. *PLoS ONE* **2016**, *11*, e0163091.

3. Pappa, F.K. & Kyriakidis, G. & Tsabaris, Christos & Patiris, Dionisis & Androulakaki, E.G. & Kaberi, Helen & Zervakis, Vassilis & Kokkoris, M. & Vlastou, R. & Krasakopoulou, Evangelia. (2019). Temporal variation of <sup>137</sup>Cs profiles in Lemnos deep basin, North Aegean Sea, Greece. HNPS Proceedings. 23. 79. 10.12681/hnps.1910.
4. Traganos D, Reinartz P. Mapping Mediterranean seagrasses with Sentinel-2 imagery. *Mar Pollut Bull.* **2018**;134:197-209. doi:10.1016/j.marpolbul.2017.06.075
5. Traganos, D.; Aggarwal, B.; Poursanidis, D.; Topouzelis, K.; Chrysoulakis, N.; Reinartz, P. Towards Global-Scale Seagrass Mapping and Monitoring Using Sentinel-2 on Google Earth Engine: The Case Study of the Aegean and Ionian Seas. *Remote Sens.* **2018**, *10*, 1227.
6. Topouzelis, Konstantinos & Makri, Despoina & Katsanevakis, Stelios & Papakonstantinou, Apostolos & Stoupas, Nikolaos. (2018). Seagrass mapping in Greek territorial waters using Landsat-8 satellite images. *International Journal of Applied Earth Observation and Geoinformation.* 67. 10.1016/j.jag.2017.12.013.

## Bibliography

1. Congedo Luca (2016). Semi-Automatic Classification Plugin Documentation. DOI: <http://dx.doi.org/10.13140/RG.2.2.29474.02242/1>
2. Immordino, Francesco & Barsanti, Mattia & Candigliota, Elena & Cocito, Silvia & Delbono, Ivana & Peirano, Andrea. (2019). Application of Sentinel-2 Multispectral Data for Habitat Mapping of Pacific Islands: Palau Republic (Micronesia, Pacific Ocean).
3. Koedsin, W.; Intararuang, W.; Ritchie, R.J.; Huete, A. An Integrated Field and Remote Sensing Method for Mapping Seagrass Species, Cover, and Biomass in Southern Thailand. *Remote Sens.* **2016**, *8*, 292.
4. Lyons, Mitchell & Roelfsema, Chris & Kennedy, Emma & Kovacs, Eva & Borrego - Acevedo, Rodney & Markey, Kathryn & Roe, Meredith & Yuwono, Doddy & Harris, Daniel & Phinn, Stuart & Asner, Gregory & Li, Jiwei & Knapp, David & Fabina,

- Nicholas & Larsen, Kirk & Traganos, Dimos & Murray, Nicholas. (2020). Mapping the world's coral reefs using a global multiscale earth observation framework. *Remote Sensing in Ecology and Conservation*. 10.1002/rse2.157.
5. Dong Jiang, Mengmeng Hao and Jingying Fu (September 14th 2016). Monitoring the Coastal Environment Using Remote Sensing and GIS Techniques, *Applied Studies of Coastal and Marine Environments*, Maged Marghany, IntechOpen, DOI: 10.5772/62242. Available from: <https://www.intechopen.com/books/applied-studies-of-coastal-and-marine-environments/monitoring-the-coastal-environment-using-remote-sensing-and-gis-techniques>
  6. Traganos, Dimos & glavan, jane & Panyawai, Janmanee & Creed, Joel & Weatherdon, Lauren & McKenzie, Len & Stankovic, Milica & Sagawa, Tatsuyuki & Komatsu, Teruhisa & Poursanidis, Dimitris. (2020). *Seagrass Mapping and Monitoring*.
  7. Hossain, Mohammad & Hashim, Mazlan. (2019). Potential of Earth Observation (EO) technologies for seagrass ecosystem service assessments. *International Journal of Applied Earth Observation and Geoinformation*. 77. 15-29. 10.1016/j.jag.2018.12.009.
  8. Han, Xingxing & Chen, Xiaoling & Feng, Lian. (2015). Four decades of winter wetland changes in Poyang Lake based on Landsat observations between 1973 and 2013. *Remote Sensing of Environment*. 156. 426-437. 10.1016/j.rse.2014.10.003.